AXONAL COLLATERALIZATION OF PRINCIPAL BASOLATERAL AMYGDALA NEURONS

*IAN T KIM, ICNELIA HUERTA-OCAMPO, OSMALYN URENA, RYO YAMAMOTO, DENIS PARE, CMBN, Rutgers University, Newark, NJ.

SfN 2023

ABSTRACT

The basolateral complex of the amygdala (**BLA**) projects to a diverse array of cortical and subcortical sites through which it influences multiple functions. Although some BLA neurons have branching axons to multiple sites, some BLA targets appear to be innervated by BLA neurons with non-branching axons.

At present, the collateralization patterns of BLA neurons remain poorly understood, largely because of technical limitations associated with retrograde tracing methods and the sheer number of possible combinations of target areas. Yet, the extent to which BLA neurons contribute axon collaterals to multiple sites is key for understanding how coding and projection site are related. For instance, it is possible that the BLA contributes multiple output streams, some of which recruit many targets that act in concert because they receive collateralizing BLA axons, while others are engaged independently because the BLA axons contacting them do not collateralize.

To shed light on this question, we adopted an intersectional recombinase-based viral tracing strategy that allows visualization of the axon collaterals contributed by different projection-defined BLA subpopulations. We found that BLA neurons projecting to the medial prefrontal cortex (**mPFC**), dorsal striatum (**dStr**), and anterior insular cortex (**AIC**), but not the ventral subiculum (**vSBC**) or ventromedial hypothalamus (**VMH**) send massive collateral projections to a common array of subcortical structures including nucleus accumbens (**nAc**), the olfactory tubercle (**OT**), nucleus of the lateral olfactory tract (**NLOT**), interstitial nucleus of the posterior limb of the anterior commissure (**IPAC**), and bed nucleus of the stria terminalis (**BNST**).

Ongoing experiments involving the injection of distinct retrograde fluorescent tracers in these structures are so far consistent with the results of the viral tracing. For instance, some of the BLA cells projecting to the mPFC or dStr also project to NLOT.

Finally, using optogenetic techniques and in vitro whole-cell recordings, we ascertained that the collateralizing axons are not passing fibers but that they form glutamatergic synapses.

Overall, the collateralization patterns we observed indicate that while some BLA targets receive inputs from BLA neurons with non-branching axons, others are innervated by BLA neurons with axons collateralizing to a hitherto underestimated array of targets. Therefore, some BLA functions may depend on the coordinated recruitment of different subsets of BLA targets.

QUESTION ADDRESSED HERE

The BLA projects to a diverse array of cortical and subcortical sites through which it influences multiple functions. There is disagreement in the literature regarding the extent to which BLA axons collateralize. However, it is possible that the discrepancy between earlier studies resulted from the fact that some BLA targets receive inputs from BLA neurons with non-branching axons whereas others are innervated by BLA cells with axon collaterals to multiple sites.

Conventional retrograde tracing methods are poorly suited to settle this question for two reasons. First, they force investigators into a compromise: the tracer volume must be sufficiently high to expose as many cells to the tracer as possible, but low enough to avoid tracer diffusion to adjacent regions. This is particularly problematic when the tracers are injected in nearby structures. Second, because the BLA projects to so many sites, there are literally hundreds of possible combinations of tracer injection sites.

WHAT WE DID

To circumvent these difficulties, we adopted an intersectional recombinase-based viral tracing strategy that allows visualization of the axon collaterals contributed by different projection-defined BLA subpopulations. We then sought corroboration of the findings obtained with viral tracing using retrograde tracing techniques. Last, we used in vitro whole-cell recordings combined with optogenetics to verify whether the axon collaterals of BLA neurons are passing axons or they form functional synapses.

Abbreviations:

OFC: orbitofrontal cortex, **AON**: anterior olfactory nucleus, **CI**: claustrum, **Endo**: endopiriform nucleus, **CeA**: central amygdala, **vHipp**: ventral hippocampus, **PeriI**: perirhinal cortex, **Ent**: entorhinal cortex, **AC**: anterior commissure, **Pir**: piriform cortex, **RS**: rhinal sulcus, **CC**: corpus callosum, **MS**: medial septum, **HF**: hippocampal formation, **PU**: putamen, **ot**: optic tract, **PVT**: paraventricular thalamus, **CMT**: centromedial thalamus, **IAM**: interoanteromedial thalamus, **SM**: stria medullaris of the thalamus, **MD**: mediodorsal thalamus, **AD**: antero-dorsal thalamus, **VA**: ventral anterior thalamus, **IC**: internal capsule, **CL**: centrolateral thalamus, **VM**: ventromedial thalamus, **RE**: nucleus reuniens.

METHODS

Viral tracing experiments

To label the axon collaterals of projection-defined BLA cells, we infused two viruses: (1) a retrograde adeno-associated virus (**AAV**) driving the expression of cre-recombinase in neurons projecting to the infusion site (AAVrg.pgk.cre; Addgene) and (2) an AAV driving expression of the fluorescent reporter tdTomato in cells expressing Cre-recombinase (AAV1.CAG.FLEX.tdTomato). Depending on the experiment, the first virus was infused in the mPFC (n=4), dStr (n=4), AIC (n=4), SBC (n=2), or VMH (n=2). The second virus was always infused in the BLA.

To further restrict the possibility that the axon collaterals we observed were due to the uptake of the viruses by non-BLA cells, in another group of rats, we used an intersectional approach that required BLA cells to express both Cre and Flp for expression of the fluorescent reporter. In these tests, the first virus was unchanged while the second virus was replaced with a combination of AAVs driving the expression of Flp (AAV.EF1a.Flpo) and of the fluorescent reporter EYFP in neurons expressing Cre and Flp (AAV8.hSyn.Con/Fon.EYFP). With both strategies, retrobeads of the opposing (green vs. red) color to the fluorophore were co-infused with the retrograde AAV to mark the infusion site.

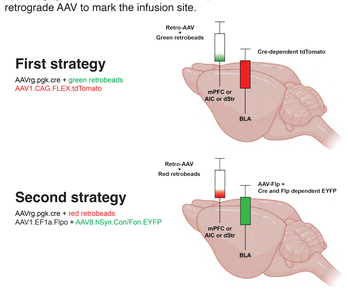

Figure 1. Retrograde AAV were infused into a BLA target area (e.g. mPFC, dStr) in both strategies, with the Cre-dependent red fluorophore tdTomato used to label BLA axons in the first strategy and Cre- and Flp-dependent green fluorophore EYFP for the second strategy.

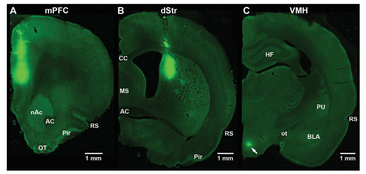

Figure 2. Examples of green retrobeads injections performed in the (**A**) mPFC, (**B**) dStr, and (**C**) VMH. The green retrobeads were co-infused with the retrograde virus we used to drive Cre expression in BLA neurons. Arrow in (**C**) points to a deposit of green retrobeads in the VMH.

Retrograde tracing experiments

To verify the results of our viral tracing experiments, we also performed experiments with conventional retrograde tracers. We used the following tracers: Fast Blue (**FB**; Polysciences, Warrington, PA), red retrobeads (**RR**, LumaFluor, Durham, NC), and Cholera Toxin B subunit (**CTB**; Sigma-Aldrich, St-Louis, MO). Various combinations of targets were tested, counterbalancing the type of tracer injected in the different target regions.

In vitro optogenetic experiments

We tested whether collateralizing axons form glutamatergic synapses using optogenetic techniques and whole-cell recordings in vitro. To this end, rats received infusions of the retrograde AAV (AAVrg.pgk.cre or AAVrg.hSyn.cre; Addgene) in a BLA target area, and of an AAV driving either the expression of the excitatory opsin Channelrhodopsin and the EYFP reporter (AAV9.EF1a.DIO.hChR2.EYFP; Addgene) or the Chronos opsin and GFP (AAV5.EF1a.FLEX.Chronos.GFP; UNC Vector Core) in cells expressing Cre in BLA.

Electrophysiological experiments were conducted two to six weeks after the virus infusions to allow for strong expression of the transgenes. Coronal slices of the BNST or NLOT were then prepared. Whole-cell current clamp recordings of potential target neurons were obtained. BLA axons were activated by blue light stimuli (5 ms; 460 nm). We ascertained that evoked responses were monosynaptic by adding tetrodotoxin (**TTX**) and 4-Aminopyridine (**4AP**) to the perfusate.

RESULTS

BLA neurons projecting to mPFC, AIC, and dStr contribute collateral projections to a common array of subcortical structures

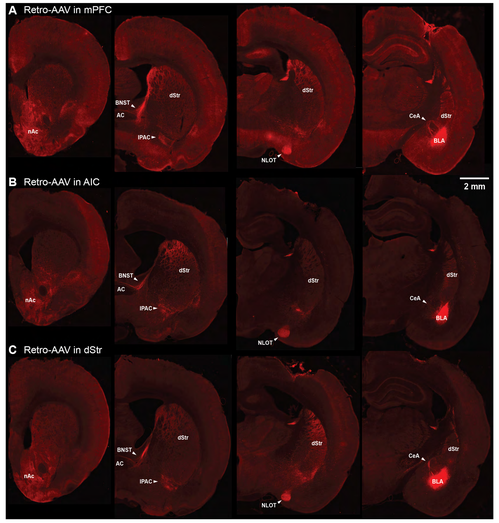

Figure 3. Collateral projections of BLA cells targeting the (**A**) mPFC, (**B**) AIC, and (**C**) dStr. (**A-C**) show coronal sections arranged from rostral (left) to caudal (right) at roughly corresponding rostro-caudal levels. Scale bar in panel (**A, right**) applies to all panels.

Collateral projections do not originate from the midline thalamus

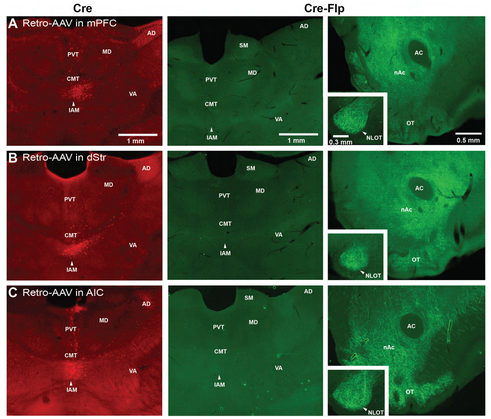

Figure 4. Many midline thalamic neurons are retrogradely labeled by the first intersectional viral tracing strategy. This was true whether the retrograde AAV was infused in the mPFC (**A, left**), dStr (**B, left**), or AIC (**C, left**). When we switched the second virus (infused into the BLA) to one requiring cells to express Cre and Flp for expression of the fluorescent reporter, no retrograde labeling is seen in the midline thalamic nuclei (**A-C, middle column**). Yet, in the same rats, we continued to observe strong collateral labeling (**A-C, right column**). Scale bars in (**A**) apply to (**B**) and (**C**).

BLA neurons projecting to the vSBC or VMH contribute few, if any, collaterals to the sites innervated by BLA cells projecting to mPFC, AIC, and dStr

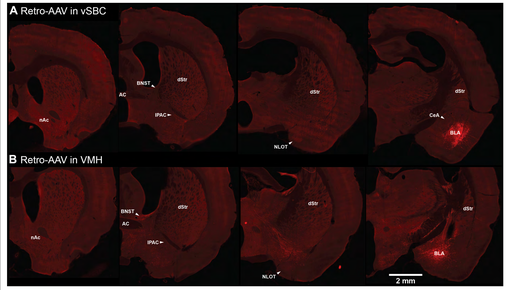

Figure 5. Collateral projections of BLA cells targeting the (**A**) vSBC and (**B**) VMH. (**A-B**) show coronal sections arranged from rostral (left) to caudal (right) at roughly corresponding rostro-caudal levels. Scale bar in panel (**B, right**) applies to all panels.

Retrograde tracing experiments corroborate the result obtained with viral tracing

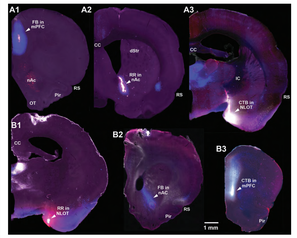

Figure 6. Examples of retrograde tracer injections in two different rats. (**A**) This rat received infusions of (**A1**) FB in mPFC, of (**A2**) RR in nAc, and of (**A3**) CTB in NLOT. (**B**) This rat received infusions of (**B1**) RR in NLOT, of (**B2**) FB in nAc, and of (**B3**) CTB in mPFC.

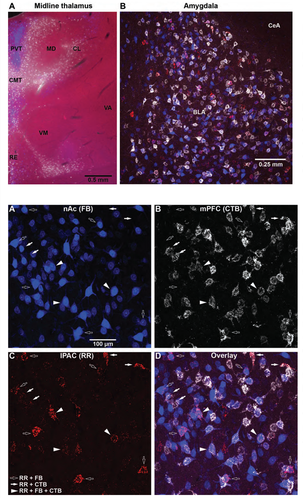

Figure 7. Contrasting distribution of (**A**) midline thalamic and (**B**) BLA cells projecting to different sites. In this rat, FB was infused in nAc, CTB in mPFC, and RR in NLOT. In the (**A**) midline thalamic region, we observed very few NLOT projecting (red) neurons, and FB labeled cells were largely confined to PVT, whereas neurons projecting to mPFC were distributed widely. In the (**B**) BLA, we observed extensive intermingling of cells projecting to the three sites.

Figure 8. Examples of retrogradely labeled BLA neurons. As indicated at the top of the panels, this rat received infusions of (**A**) FB in nAc, (**B**) CTB in mPFC, and (**C**) RR in NLOT. BLA neurons labeled with each of these tracers are shown in (**A-C**), respectively. (**D**) Overlay of the blue, white, and red channels, revealing the presence of cells labeled by one, two, or three of the tracers. As indicated at the bottom of (**C**), **black arrows** point to neurons retrogradely labeled with RR and FB, **white arrows** point to neurons retrogradely labeled with RR and CTB, and the **triangle arrowheads** point to neurons labeled with all three tracers.

NLOT, mPFC, nAc

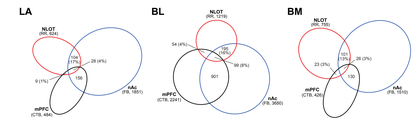

IPAC, mPFC, nAc

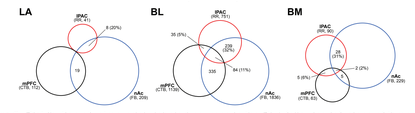

Figure 9. Distribution of retrogradely labeled neurons in the BLA following infusions of three retrograde tracers in various BLA targets. The percentages are based on the total number of labeled BLA neurons that project to either NLOT or IPAC.

The axon collaterals of BLA neurons are not passing fibers; they form functional glutamatergic synapses

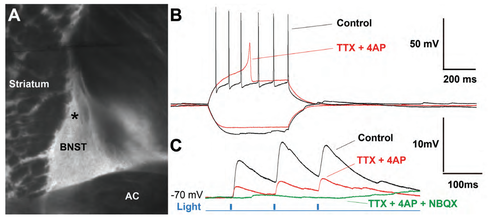

Figure 10. Retrograde AAV infused in mPFC. BLA received infusion of AAV5.EF1a.FLEX.Chronos.GFP. (**A**) GFP-labeled axons in BNST. *Asterisk:* position of recorded cell. (**B**) Voltage responses to current pulses before (black) and after addition of TTX + 4AP (red). (**C**) Responses to blue light stimuli before (black) and after addition of TTX + 4AP (red) and then TTX + 4AP + NBQX (green) to the perfusate.

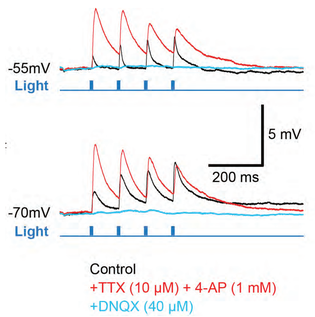

Figure 11. Retrograde AAV was infused in nAc. BLA was infused with AAV9.EF1a.DIO.hChR2.EYFP. Responses in NLOT to blue light pulses were evoked from -55 mV (**top**) or -70 mV (**bottom**) before (black) and after addition of TTX + 4AP (red) and then TTX + 4AP + DNQX (light blue) to the perfusate.

SUMMARY AND CONCLUSIONS

Overall, the collateralization patterns we observed indicate that while some BLA targets receive inputs from BLA neurons with non-branching axons, others are innervated by BLA neurons with axons collateralizing to a hitherto underestimated array of common targets. Therefore, some BLA functions may depend on the coordinated recruitment of different subsets of BLA targets.

ACKNOWLEDGEMENTS

This material is based upon work supported by grant MH-112505 to DP from NIMH and BNS graduate program funding to ITK.